

# Design of a novel freeform lens for LED uniform illumination and conformal phosphor coating

Run Hu,<sup>1,2</sup> Xiaobing Luo,<sup>1,2,\*</sup> Huai Zheng,<sup>1,2</sup> Zong Qin,<sup>3</sup> Zhiqiang Gan,<sup>3</sup> Bulong Wu,<sup>2</sup> and Sheng Liu<sup>1,4</sup>

<sup>1</sup>Wuhan National Laboratory for Optoelectronics, Huazhong University of Science and Technology, Wuhan, 430074, China

<sup>2</sup>School of Energy and Power Engineering, Huazhong University of Science and Technology, Wuhan, 430074, China

<sup>3</sup>School of Optoelectronic Science and Engineering, Huazhong University of Science and Technology, Wuhan, 430074, China

<sup>4</sup>School of Mechanical Science and Engineering, Huazhong University of Science & Technology, Wuhan, 430074, China

\*luoxb@mail.hust.edu.cn

**Abstract:** A conformal phosphor coating can realize a phosphor layer with uniform thickness, which could enhance the angular color uniformity (ACU) of light-emitting diode (LED) packaging. In this study, a novel freeform lens was designed for simultaneous realization of LED uniform illumination and conformal phosphor coating. The detailed algorithm of the design method, which involves an extended light source and double refractions, was presented. The packaging configuration of the LED modules and the modeling of the light-conversion process were also presented. Monte Carlo ray-tracing simulations were conducted to validate the design method by comparisons with a conventional freeform lens. It is demonstrated that for the LED module with the present freeform lens, the illumination uniformity and ACU was 0.89 and 0.9283, respectively. The present freeform lens can realize equivalent illumination uniformity, but the angular color uniformity can be enhanced by 282.3% when compared with the conventional freeform lens.

©2012 Optical Society of America

**OCIS codes:** (230.3670) Light-emitting diodes; (220.3630) Lenses; (220.2945) Illumination design; (350.4600) Optical engineering.

---

## References and links

1. S. Pimputkar, J. S. Speck, S. P. Denbaars, and S. Nakamura, "Prospects for LED lighting," *Nat. Photonics* **3**(4), 180–182 (2009).
2. E. F. Schubert and J. K. Kim, "Solid-state light sources getting smart," *Science* **308**(5726), 1274–1278 (2005).
3. S. Tonzani, "Lighting technology: Time to change the bulb," *Nature* **459**(7245), 312–314 (2009).
4. Z. Y. Liu, S. Liu, K. Wang, and X. B. Luo, "Status and prospects for phosphor-based white LED packaging," *Front. Optoelectron. China* **2**, 119–140 (2009).
5. N. Narendran, "Is solid-state lighting ready for the incandescent lamp phase-out?" *Proc. SPIE* **8123**, 812302 (2011).
6. S. Liu and X. B. Luo, *LED Packaging for Lighting Applications: Design, Manufacturing and Testing* (John Wiley & Sons, 2011).
7. K. Wang, F. Chen, Z. Y. Liu, X. B. Luo, and S. Liu, "Design of compact freeform lens for application specific light-emitting diode packaging," *Opt. Express* **18**(2), 413–425 (2010).
8. P. Benítez, J. C. Miñano, J. Blen, R. Mohedano, J. Chaves, O. Dross, M. Hernández, and W. Falicoff, "Simultaneous multiple surface optical design method in three dimensions," *Opt. Eng.* **43**(7), 1489–1502 (2004).
9. J. C. Miñano, P. Benítez, J. Y. Liu, J. Infante, J. Chaves, and W. Lin, "Applications of the SMS method to design of compact optics," *Proc. SPIE* **7717**, 771701 (2010).
10. H. Ries and J. Muschaweck, "Tailoring freeform lenses for illumination," *Proc. SPIE* **4442**, 43–50 (2001).
11. Y. Ding, X. Liu, Z. R. Zheng, and P. F. Gu, "Freeform LED lens for uniform illumination," *Opt. Express* **16**(17), 12958–12966 (2008).
12. K. Wang, S. Liu, F. Chen, Z. Qin, Z. Y. Liu, and X. B. Luo, "Freeform LED lens for rectangularly prescribed illumination," *J. Opt. A, Pure Appl. Opt.* **11**(10), 105501 (2009).
13. L. Wang, K. Qian, and Y. Luo, "Discontinuous free-form lens design for prescribed irradiance," *Appl. Opt.* **46**(18), 3716–3723 (2007).

14. K. Wang, D. Wu, Z. Qin, F. Chen, X. B. Luo, and S. Liu, "New reversing design method for LED uniform illumination," *Opt. Express* **19**(Suppl 4), A830–A840 (2011).
15. F. Chen, S. Liu, K. Wang, Z. Y. Liu, and X. B. Luo, "Free-form lenses for high illuminance quality light-emitting diode MR16 lamps," *Opt. Eng.* **48**(12), 123002 (2009).
16. F. Chen, K. Wang, Z. Qin, D. Wu, X. B. Luo, and S. Liu, "Design method of high-efficient LED headlamp lens," *Opt. Express* **18**(20), 20926–20938 (2010).
17. Z. Qin, K. Wang, F. Chen, X. B. Luo, and S. Liu, "Analysis of condition for uniform lighting generated by array of light emitting diodes with large view angle," *Opt. Express* **18**(16), 17460–17476 (2010).
18. S. Wang, K. Wang, F. Chen, and S. Liu, "Design of primary optics for LED chip array in road lighting application," *Opt. Express* **19**(Suppl 4), A716–A724 (2011).
19. C. Sommer, P. Hartmann, P. Pachler, M. Schweighart, S. Tasch, G. Leising, and F. P. Wenzl, "A detailed study on the requirements for angular homogeneity of phosphor converted high power white LED light sources," *Opt. Mater.* **31**(6), 837–848 (2009).
20. K. Wang, D. Wu, F. Chen, Z. Y. Liu, X. B. Luo, and S. Liu, "Angular color uniformity enhancement of white light-emitting diodes integrated with freeform lenses," *Opt. Lett.* **35**(11), 1860–1862 (2010).
21. W. D. Collins, M. R. Krames, G. J. Verhoeckx, and N. J. M. Leth, "Using electrophoresis to produce a conformal coated phosphor-converted light emitting semiconductor," US Patent 6576488 (2001).
22. B. Hou, H. B. Rao, and J. F. Li, "Phosphor coating technique with slurry method in application of white LED," *Proc. SPIE* **6841**, 684106 (2007).
23. J. H. Yum, S. Y. Seo, S. Lee, and Y. E. Sung, "Comparison of  $Y_3Al_4O_{12}:Ce_{0.05}$  phosphor coating methods for white light-emitting diode on gallium nitride," *Proc. SPIE* **4445**, 60–69 (2001).
24. B. P. Loh, N. W. Medendorp, Jr., P. Andrews, Y. Fu, M. Laughner, and R. Letoquin, "Method of uniform phosphor chip coating and LED package fabricated using method," US Patent 20080079017 A1 (2008).
25. B. Braune, K. Petersen, J. Strauss, P. Kromotis, and M. Kaempf, "A new wafer level coating technique to reduce the color distribution of LEDs," *Proc. SPIE* **6486**, 64860X (2007).
26. H. Zheng, X. B. Luo, R. Hu, B. Cao, X. Fu, Y. M. Wang, and S. Liu, "Conformal phosphor coating using capillary microchannel for controlling color deviation of phosphor-converted white light-emitting diodes," *Opt. Express* **20**(5), 5092–5098 (2012).
27. L. Piegl and W. Tiller, *The NURBS Book*, 2nd ed. (Springer, 1996).
28. Z. Y. Liu, K. Wang, X. B. Luo, and S. Liu, "Precise optical modeling of blue light-emitting diodes by Monte Carlo ray-tracing," *Opt. Express* **18**(9), 9398–9412 (2010).
29. R. Hu, X. B. Luo, and S. Liu, "Study on the optical properties of conformal coating light-emitting diode by Monte Carlo simulation," *IEEE Photon. Technol. Lett.* **23**(22), 1673–1675 (2011).
30. C. Sommer, F. Reil, J. R. Krenn, P. Hartmann, P. Pachler, H. Hoschopf, and F. P. Wenzl, "The impact of light scattering on the radiant flux of phosphor-converted high power white light-emitting diodes," *J. Lightwave Technol.* **29**(15), 2285–2291 (2011).
31. C. Sommer, F. P. Wenzl, P. Hartmann, P. Pachler, M. Schweighart, S. Tasch, and G. Leising, "Tailoring of the color conversion elements in phosphor-converted high-power LEDs by optical simulations," *IEEE Photon. Technol. Lett.* **20**(9), 739–741 (2008).
32. Z. Y. Liu, S. Liu, K. Wang, and X. B. Luo, "Measurement and numerical studies of optical properties of YAG:Ce phosphor for white light-emitting diode packaging," *Appl. Opt.* **49**(2), 247–257 (2010).
33. R. Hu, X. B. Luo, H. Feng, and S. Liu, "Effect of phosphor settling on the optical performance of phosphor-converted white light-emitting diodes," *J. Lumin.* **132**(5), 1252–1256 (2012).
34. Z. Y. Liu, S. Liu, K. Wang, and X. B. Luo, "Optical analysis of color distribution in white LEDs with various packaging methods," *IEEE Photon. Technol. Lett.* **20**(24), 2027–2029 (2008).

## 1. Introduction

Compared with traditional light sources, a white light-emitting diode (LED) has many advantages, such as high luminous efficiency, low power consumption, high reliability, and long life. Thus, LEDs are considered as a strong candidate for the next-generation light source and gradually are becoming widely used in our daily lives [1–5]. However, the direct output of an LED is usually a circle spot with non-uniform illuminance distribution, which makes it hard to meet the illumination requirement. Therefore, LED luminaries are generally required to re-distribute the spatial distribution of the LED's light energy through appropriate primary or secondary optics so that the light pattern and uniformity can be controlled for high-quality LED illumination [6,7]. A freeform lens is a type of newly emerging, non-imaging optics and has become a trend in LED optics design due to its advantages in abundant design freedom, compact size, and accurate light control. There exist many methods to deal with freeform lens design: the simultaneous multiple surface (SMS) method [7,8], the tailored freeform surface method [9], partial differential equations [10], the discontinuous freeform lens method [11–13], and the continuous freeform lens method [7,14–18]. These design methods, except for the SMS method, usually deal with the outer surface, and the inner surface is considered as a hemispherical shape for simplicity, which would abandon important design freedom in the

inner surface of a freeform lens. Although the SMS method could deal with multiple freeform surfaces simultaneously by controlling the light directions, it is too complicated and could not guarantee the uniformity of the light–energy distribution.

On the other hand, uniform illumination is not the only requirement for high light quality of LED packaging; high angular color uniformity (ACU) is also required in many applications [19,20]. In the conventional phosphor-dispensing method, the geometry of the phosphor layer is usually convex, which leads to low ACU in the whole radiation angle. To overcome the poor ACU of the conventional phosphor-dispensing method, the conformal coating method was proposed in which the thickness of the phosphor layer is uniform. Currently, there are many methods to realize conformal coating: electrophoresis [21], slurry [22], settling [23], evaporating solvent [24], wafer-level coating [25], and capillary-assisted coating [26], for example. All of these methods have pros and cons—basically, they all need extra-process sequences or extra-process requirements to coat the phosphor layer onto the chip uniformly, and some of process sequences are difficult and some of the requirements are rigorous. Therefore, people both in industry and in academia still spend a lot of effort on the development of conformal phosphor-coating technology.

High-quality LED illumination, which requires high illumination uniformity, high ACU, and precise light pattern control, is in great demand by consumers and markets. Therefore, an optic design that can realize these requirements simultaneously has become a development trend. In this study, we designed a novel freeform lens for LED uniform illumination as well as realization of a conformal phosphor coating. The algorithm of the method involving the extended light source is presented in detail. The lighting performance of the present freeform lens is validated. Both the illumination uniformity and ACU were examined by Monte Carlo ray-tracing simulations.

## 2. Problem statement

As shown in Fig. 1(a), regardless of whether in the conventional freeform lens or in the hemispherical lens, the inner surface is hemispherical, which can make the lens design convenient and effective for a point light source. In order to coordinate the laying of conventional lenses in existing LED packaging processes, after the phosphor silicone matrix is dispersed onto the chip, silicone is put in the interspace between the substrate and the lens to expel the air and to protect the chips and the bonding wires. In these packaging processes, the non-uniform phosphor layer may lead to poor ACU in the whole radiation angle. On the other hand, the main advantage of the conformal phosphor coating lies in the uniform thickness of the phosphor layer.

Inspired by the existing packaging processes and the advantage of a conformal phosphor coating, one possible idea comes up: why not design a freeform lens in which the height of the inner surface is uniform? If so, we can realize a conformal phosphor coating by filling the interspace between the lens and the LED chip with a phosphor–silicone matrix. As shown in Fig. 1(b), if the inner surface of the freeform lens is flat, the thickness of the phosphor layer is uniform; thus, a conformal phosphor coating is realized.

With such a novel freeform lens, the packaging processes in the industry may even be facilitated and simplified. As shown in Fig. 1, the silicone-filling process can be integrated with the phosphor-coating process. After the novel lens is mounted, a phosphor–silicone matrix is filled into the interspace, which not only can realize a conformal phosphor coating, but also can play the role of silicone to protect the chip and bonding wires. If such a freeform lens is feasible, we can save packaging time and cost and improve manufacturing efficiency.

To design such a freeform lens with a uniform-height inner surface, we are faced with two inevitable problems. One is light control when the rays are refracted by the inner and outer surfaces through the lens; the other is the extended light source. The double refractions on the two surfaces make light control difficult, which should be designed well by considering the full light path from the light source to the target plane simultaneously. Since the thickness of the conformal phosphor coating layer is usually small, the LED chip could not be considered

as a point light source any longer. The detailed design method is presented in the following sections.

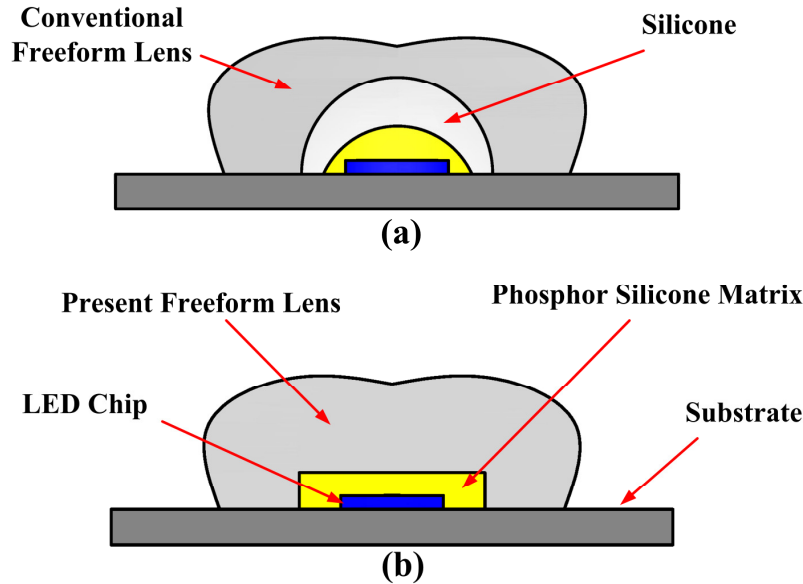


Fig. 1. (a) LED packaging module with conventional freeform lens, and (b) LED packaging module with novel freeform lens applied to conformal phosphor coating.

### 3. Design method for freeform lens for conformal coating

The design method consists of two main steps:

1. Establishing the light–energy mapping relationship between the light source and the target plane.
2. Constructing the freeform lens. A circular target plane is adopted as the example in the following design, but the design method can also be extended to other target planes, such as a rectangular plane.

#### 3.1 Establishing the light–energy mapping relationship

As shown in Fig. 2, the energy distribution of the light source is divided into  $M \times N$  grids with equal luminous flux, where the latitude is divided into  $N$  parts and the longitude is divided into  $M$  parts. Due to the central symmetry of the energy distribution of the light source, the light energy of each grid at the same latitude is the same. Then we can integrate the  $N$  grids along the latitude together and just consider the  $M$  parts along the longitude. According to the principle of photometry, the luminous flux of the unit area of the  $M$  parts  $\Phi(\theta)$  and the total light source  $\Phi_{total}$  can be calculated as Eq. (1) and Eq. (2), respectively.

$$\Phi(\theta) = \int_0^{2\pi} \int_{\theta_i}^{\theta_{i+1}} I(\theta, \varphi) \sin \theta d\theta d\varphi, \quad (1)$$

$$\Phi_{total} = \int_0^{\pi/2} \Phi(\theta) d\theta, \quad (2)$$

where  $I(\theta)$  is the light intensity, and  $\theta$  and  $\varphi$  are the notions shown in Fig. 2. The edge angle  $\theta_i$  ( $i = 1, 2, \dots, M$ ) of each part, which defines the direction of edge light of each source grid, can be calculated by Eq. (3). Thus the light source is divided into  $M$  parts with equal luminous flux.

$$\int_0^{\theta_i} 2\pi I(\theta) \sin \theta d\theta = i \frac{\Phi_{total}}{M}, (i = 1, 2, \dots, M). \quad (3)$$

To overcome the problem of lighting-performance deterioration caused by an extended light source and the scattering of phosphor particles, we divide the target plane into  $M$  concentric rings with unequal areas by inserting optimization coefficient  $C_i$ . For an arbitrary circle area with a radius of  $r_i$ , it is the summation of  $i$  concentric rings and we can obtain

$$\pi r_i^2 = i C_i \frac{\pi L^2}{M}, (i = 1, 2, \dots, M). \quad (4)$$

Thus the radius  $r_i$  of each concentric ring on the target plane can be calculated as

$$r_i = L \sqrt{\frac{i C_i}{M}}. \quad (5)$$

The purpose of introducing optimization coefficients is to optimize the light-energy distribution on the target plane to compensate for the illumination deterioration caused by the extended light source and the scattering of phosphor particles. The optimization coefficients must be equal to 1 when dealing with point light-source problems. During the design for the extended light source, we adjust  $C_i$  to make the trend of illumination distribution on the target plane to be the inverse of the trend of light-performance deterioration caused by the rays emanating from the edge area of the LED chip. However, it should be noted that the assignment of  $C_i$  is not arbitrary. Since the radius of the arbitrary circle area  $r_i$  is incremental, according to Eq. (5), the series  $\{i C_i\}$  must be an ascending series. The last term of the series  $M C_M$  must be the largest, and at this situation,  $r_M$  must equal to  $L$ ; thus,  $C_M$  must be 1. Therefore, each term of  $\{i C_i\}$  must be less than  $M$ . According to the edge ray principle, rays from the edge of the light source should strike the edge of the target [14]. With the above gridding method, we can establish the light-energy mapping relationship between the extended light source and the target plane. As a result, we can obtain the edge angle  $\theta_i$  and the corresponding radius  $r_i$  of each ray.

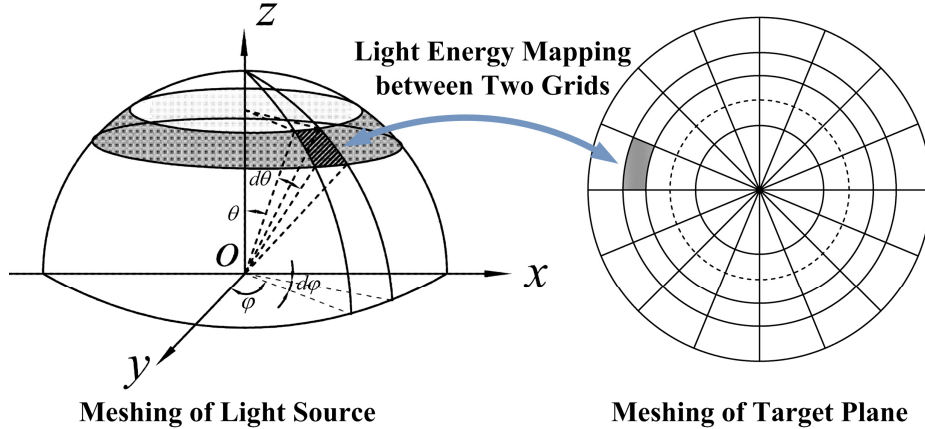


Fig. 2. Schematic of light-energy mapping between the light source and the target plane.

### 3.2 Constructing the freeform lens

Since both the target plane and the light intensity distribution of the light source are central symmetrical, the lens could also be designed as centrally symmetrical. Figure 3 shows the typical light path from the light source to the target plane through the present freeform lens. As shown in Fig. 3, the incident ray  $\overline{OA}$  is refracted to  $\overline{AB}$  by the inner surface, then  $\overline{AB}$  is refracted by the outer surface, and the output ray  $\overline{BR}$  irradiates at the corresponding point  $R$  on

the target plane. According to Snell's law, the ray  $\overline{OA}$ ,  $\overline{AB}$ , and  $\overline{BR}$  must satisfy the following equations: [6]

$$n_1 \frac{\overline{OA}}{|\overline{OA}|} \times \overline{N}_1 = n_2 \frac{\overline{AB}}{|\overline{AB}|} \times \overline{N}_1, \quad (6)$$

$$n_2 \frac{\overline{AB}}{|\overline{AB}|} \times \overline{N}_2 = n_3 \frac{\overline{BR}}{|\overline{BR}|} \times \overline{N}_2, \quad (7)$$

where  $\overline{N}_1$  and  $\overline{N}_2$  are the unit normal vectors of the inner surface and outer surface, respectively;  $n_1$ ,  $n_2$ , and  $n_3$  are the refractive indices of each area, respectively;  $n_1$  is the refractive index of the phosphor silicone matrix;  $n_2$  is the refractive index of the lens material; and  $n_3$  equals 1.00 because the area is air.

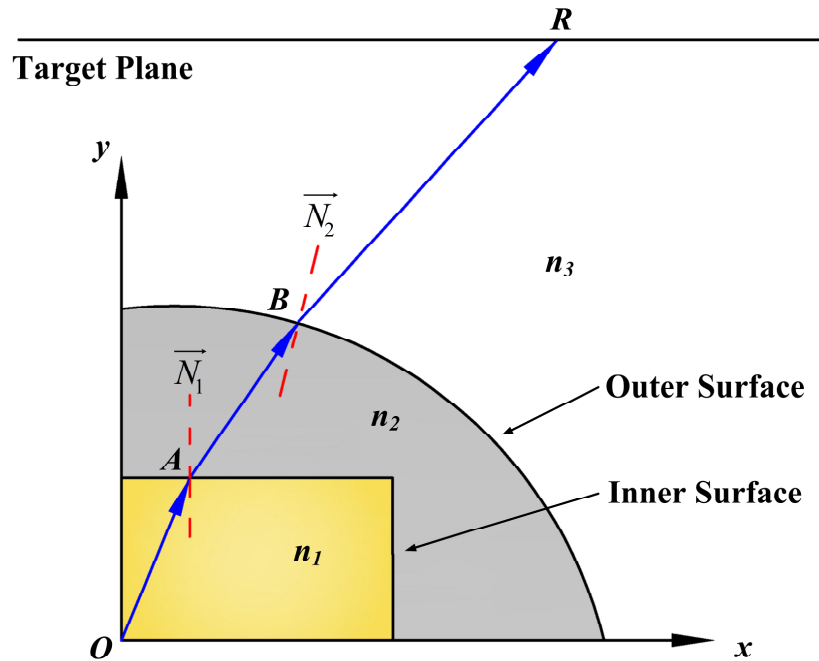


Fig. 3. Schematic of typical light path from the light source to the target plane through the present freeform lens. The inner surface is a cylinder and the outer surface is freeform.

To be more specific, in this design the inner surface is a cylinder with a radius of  $a$  and a height of  $b$ . Therefore, as shown in Fig. 4, there exists a turning point  $A_T$  on the inner surface. The edge angle of the incident ray corresponding to  $A_T$  is denoted as  $\theta_T$ , which can be determined by  $\theta_T = \arctan(a/b)$ . According to relationship between the edge angle of the incident angle  $\theta_i$  and  $\theta_T$ , the inner surface can be divided into two cases:

- Case I: when the edge angle  $\theta_i$  is less than  $\theta_T$ , the light path is illustrated as the light path of “ $O-A_i-B_i-R_i$ ”.
- Case II: when the edge angle  $\theta_j$  is larger than  $\theta_T$ , the light path is illustrated as the light path of “ $O-A_j-B_j-R_j$ ”.

In both cases, the refractions happening on the inner and outer surfaces are controlled by Snell's law, and Eq. (6) and Eq. (7) could be rewritten as Eq. (8) and Eq. (9) with the notions in Fig. 4.

$$n_1 \sin \alpha_x = n_2 \sin \beta_x, (x = i, j), \quad (8)$$

$$n_2 \sin \psi_x = n_3 \sin \omega_x, (x = i, j). \quad (9)$$

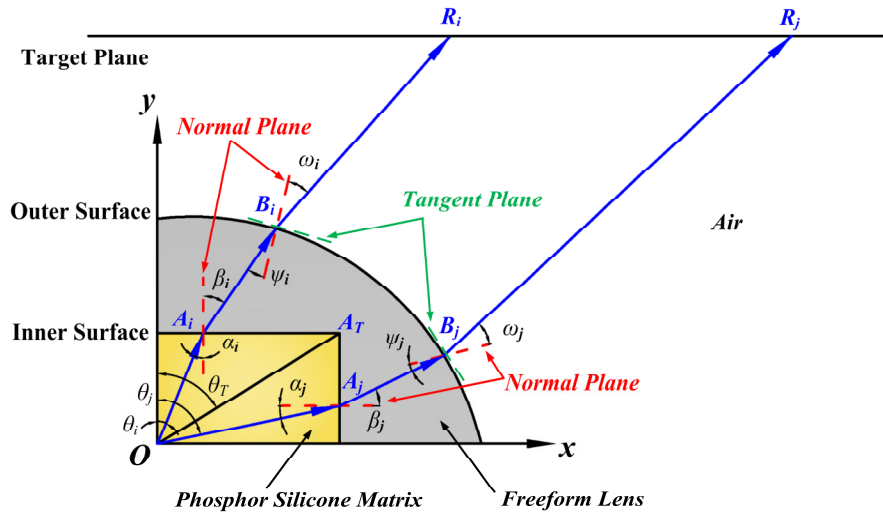


Fig. 4. Specific light paths from the light source to the target plane through the present freeform lens. Phosphor silicone matrix is filled in the interspace between the light source and inner surface of the lens. Blue lines are the typical light paths. Red dashed lines are the normal plane and green dashed lines are the tangent plane. Point  $A_T$  is the turning point of the inner surface.  $\alpha_x(x = i, j)$  and  $\beta_x(x = i, j)$  are the incident angle and refraction angle on the inner surface, respectively.  $\psi_x(x = i, j)$  and  $\omega_x(x = i, j)$  are the incident angle and refraction angle on the outer surface, respectively.

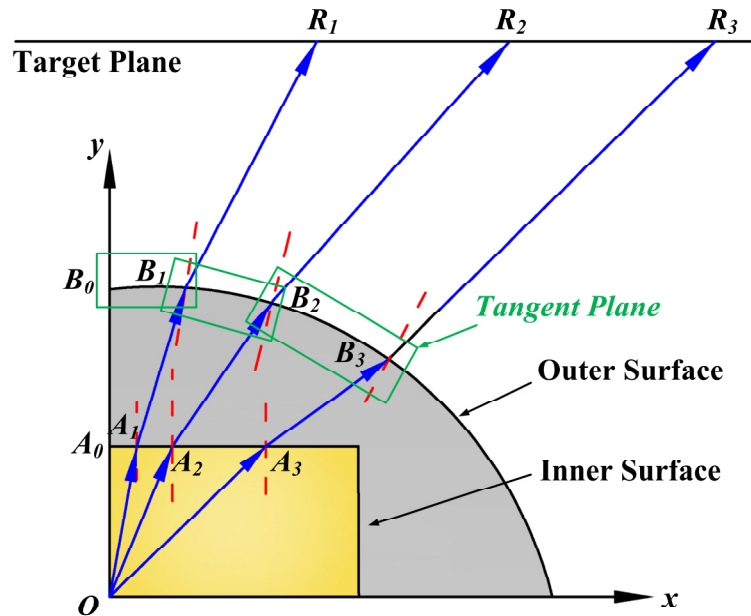


Fig. 5. Schematic of point generation on the outer surface of the present freeform lens. Red dashed lines are the normal plane and green boxes are the tangent plane of the points on the outer surface.

In *Case I*, when the inner surface is given, the coordinates of  $A_i$  can be denoted as  $(b \times \tan\theta_i, b)$ . From the geometrical relationship in Fig. 4,  $\alpha_i$  equals  $\theta_i$ ; therefore, the vector  $\overline{A_i B_i}$  can be calculated by solving  $\beta_i$  in Eq. (8). To obtain the coordinates of points  $B_i$  on the outer surface, as shown in Fig. 5, we first fix an initial point  $B_0$  as the vertex of the outer surface of the lens, and the normal vector at this point is vertical up. The second point  $B_1$  can be calculated by the intersection of the incident ray  $\overline{A_1 B_1}$  and the tangent plane of the point  $B_0$ . Since the corresponding point  $R_1$  was determined previously, according to Eq. (7), we can then calculate the unit normal vector on point  $B_1$  on the outer surface and consequently obtain the tangent plane. The tangent plane on point  $B_1$  can help obtain the coordinates of the next point  $B_2$ . By repeating this process until the edge angle  $\theta_i$  approaches  $\theta_T$ , we can get all of the points  $B_i$  and their unit normal vectors on the outer surface.

In *Case II*, the coordinates of  $A_j$  can be denoted as  $(a, a \times \cot\theta_j)$ . From Fig. 4,  $\alpha_j$  equals to  $(\pi/2 - \theta_j)$ , therefore the vector  $\overline{A_j B_j}$  can also be calculated by solving  $\beta_j$  in Eq. (8). With the similar method in *Case I*, we could obtain the coordinates of  $B_j$  on the outer surface.

After obtaining all of the coordinates of points on the outer surface, we fit these points to generate the contour line of the lens's cross section by applying the lofting method [27], and we then get the freeform lens by rotating the contour line around the symmetry axis.

#### 4. Simulation methodology

To validate the above design method, we designed a freeform lens to realize a conformal phosphor coating. As a comparison, we also built a conventional freeform lens. The lighting performance, including the illumination uniformity and the ACU of these two lenses, was examined. This section will be followed by a detailed description of simulation models, including the packaging configuration and the chip structure. Then we present the simulations process, especially the simulation of color conversion in a phosphor–silicone matrix.

##### 4.1 Model setup

As shown in Fig. 1, we built two LED module models: one with the present freeform lens and the other with the existing conventional freeform lens. It is seen that the inner surface of the present freeform lens was a cylinder and the outer surface was freeform. The radius of the cylinder was 0.8 mm and its height was 0.4 mm. The initial height of the outer surface was 2 mm. Figure 6(a) shows the specific packaging configuration of an LED module with the present freeform lens with consideration of a phosphor–silicone matrix. As mentioned above, the phosphor–silicone matrix was placed between the LED chip and the freeform lens, so therefore its shape was also cylindrical and the thickness was 0.3 mm. While in the conventional freeform lens, the outer surface was freeform while the inner surface was hemispherical. The initial height of the outer surface was also 2 mm and the radius of the inner surface was 1 mm. The material of these two lenses was selected as polymethylmethacrylate (PMMA) and its refractive index is 1.4935.

Besides the above models, we also built a precise model of the LED chip. In this study, the LED chip was a conventional GaN chip and its typical structure is shown in Fig. 6(b). The thickness and composites of different layers were sketched, and the chip size was  $1 \times 1$  mm. The luminescent multi-quantum well (MQW) was sandwiched by an n-GaN layer and a heterostructure of a p-GaN layer and a p-AlGaIn layer. A current-spreading layer fabricated by indium tin oxide (ITO) and a sapphire substrate were also taken into consideration. The top and bottom surfaces of the MQW were set as luminescent surfaces with Lambertian light distribution. The absorption coefficients and refractive indices for p-GaN, MQW, and n-GaN were 5, 8, and  $5 \text{ mm}^{-1}$  and 2.45, 2.54, and 2.42, respectively [28,29]. The reflection coefficient of the reflecting layer (Ag) was set as 0.95. By setting the absorption coefficients and refractive indices of the materials, the precise model of a conventional GaN blue LED chip could be achieved successfully.



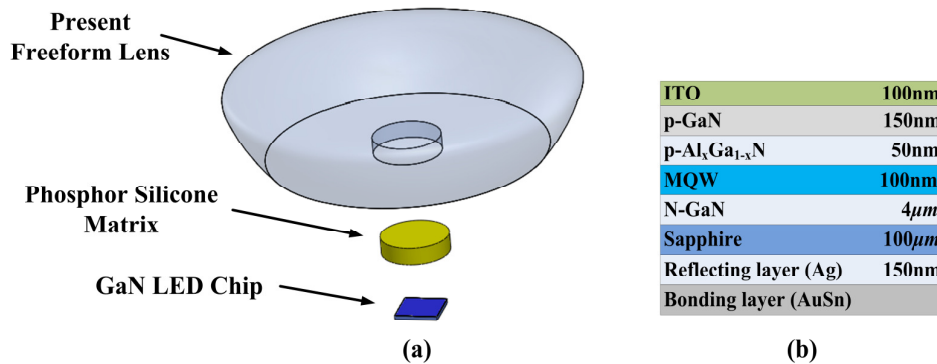


Fig. 6. (a) Packaging configuration of LED module with present freeform lens. (b) Structure of conventional GaN LED chip.

#### 4.2 Simulation process

After building the models of these two LED modules, Monte Carlo ray-tracing simulations were used to validate the lighting performance, including the illumination uniformity and the ACU. In the Monte Carlo ray-tracing simulation, 1 million rays from randomly selected points on the surfaces of the light source strike into randomly selected angles in the space. The selections of starting points and ray direction are based on probabilistic functions that describe the emissive characteristics of the light sources [6]. In all of the simulations, the distance between the light source and the target plane was 50 mm and the radius of the target plane was also 50 mm. According to the simulation results, we optimized the coefficients  $C_i$  until the lighting performance satisfied the requirements of some specific applications.

As for the simulation of a phosphor–silicone matrix, the phosphor particles can absorb part of the blue light emanating from the LED chip and re-emit a yellow light. The rest of the blue light and the yellow light can mix with each other, and white light is therefore produced. The quantum efficiency of the phosphor was assumed to be 80%, which means 0.8 photons of the converted yellow light could be re-emitted from the phosphor particle when one blue photon was absorbed by one phosphor particle [30,31]. The detailed parameters of the phosphor, especially the absorption coefficients and scattering coefficients, were obtained from the Mie theory [32,33]. The wavelength-dependent refractive indices, absorption, and scattering coefficients, which varied with the changes of phosphor concentration, played important roles in determining the optical performance of the LED packages. In this study, to make the simulation closer to reality, the phosphor concentration was set as 0.16 g/cm<sup>3</sup>. The necessary parameters in the simulations can be found in our previous works [28,29,32–34]. For modeling the light conversion process, the rays of blue and yellow light were simulated separately by the Monte Carlo ray-tracing method. In the simulation, two wavelengths were ray traced separately, namely 465 nm and 555 nm, which represent the blue LED light and the phosphor-converted yellow light, respectively [28,29]. The blue light emanated from the top surface of the chip and the yellow light was emitted from the volume of phosphor silicone matrix according to the distribution of phosphor particles inside the silicone matrix.

### 5. Results and discussions

The lighting performance comparisons between these two LED modules are shown in Fig. 7 and Fig. 8, respectively. The irradiance profiles in both results were normalized to peak irradiance. From Fig. 7 and Fig. 8, it is noticed that the bright regions in both figures are very large and the irradiance profiles are flat in the center region. The illumination uniformity was calculated as the ratio of average irradiance to the maximum irradiance, and the values were 0.89 and 0.90 in Fig. 7 and Fig. 8, respectively. It can be seen that the present freeform lens

had equivalent illumination uniformity as that of a conventional freeform lens; thus, its lighting performance could satisfy the requirements of most applications.

We introduced the yellow-blue ratio (YBR) to represent the variation of correlated color temperature (CCT) [20,29]. The higher the YBR is, the larger the yellow light intensity is and the lower CCT is. The ACU can be calculated as the minimum YBR to the maximum YBR in the whole radiation angle. The light intensities of the two LED modules are illustrated in Fig. 9. From the comparison, it is seen that the YBR curve of the LED module with the present freeform lens was much flatter. For the comparative YBR curve, the YBR increased greatly in the edge region, which may lead to a “yellow ring” at the edge of light pattern. Hence, the ACUs were 0.9283 and 0.2428 for LED modules with the present freeform lens and conventional freeform lens, respectively. The ACU was enhanced by 282.3% after using the present freeform lens. It is concluded that the ACU could be enhanced by the present freeform lens extraordinarily.

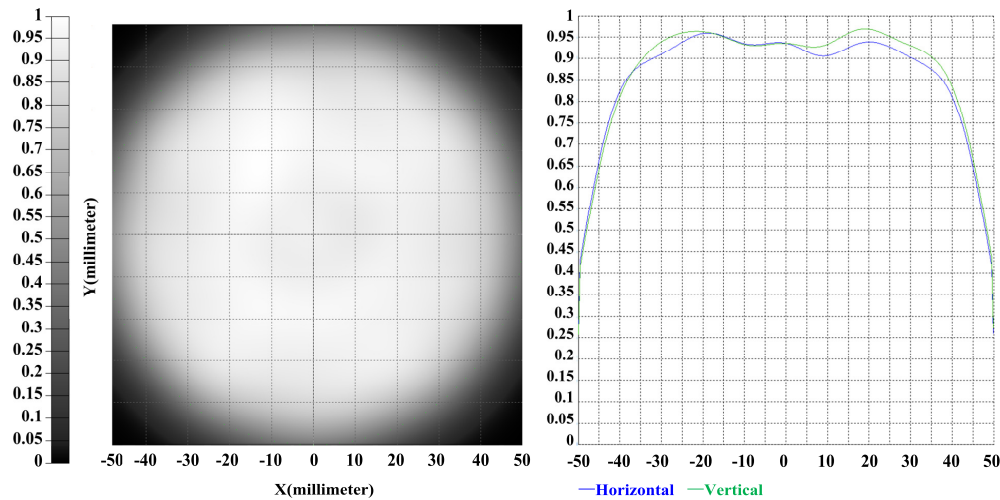


Fig. 7. Lighting performance of the present freeform lens.

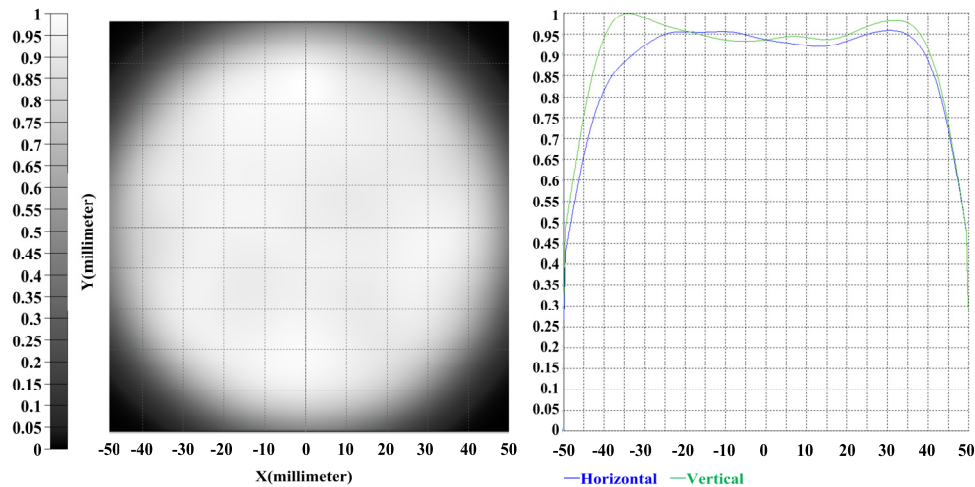


Fig. 8. Lighting performance of the conventional freeform lens.

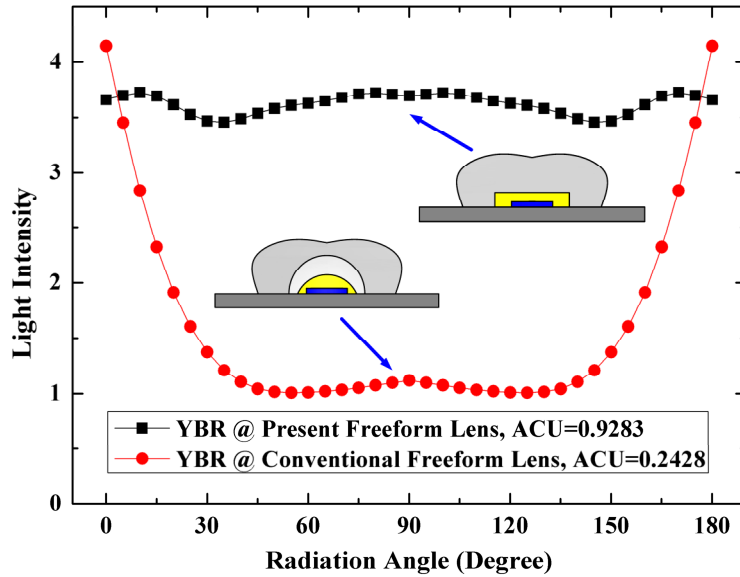


Fig. 9. Comparison of light intensity of YBR and ACU in the whole radiation angle between the LED modules with the present freeform lens and the conventional freeform lens.

## 6. Conclusions

In this study, a novel freeform lens, whose inner surface was a cylinder and whose outer surface was freeform, was designed for LED uniform illumination and realization of a conformal phosphor coating simultaneously. The algorithm of the design method was presented in detail, and Monte Carlo ray-tracing simulations were conducted for validation. By controlling the shape of the inner surface, we realized a thin conformal phosphor coating layer whose thickness was only 0.3 mm. It is demonstrated that the present freeform lens can realize equivalent illumination uniformity, but the angular color uniformity can be enhanced by 282.3% when compared with the conventional freeform lens. The illumination uniformity and angular color uniformity of the LED module with the present freeform lens were 0.89 and 0.9283, respectively.

## Acknowledgments

The authors acknowledge the financial support in part from the 973 Project of The Ministry of Science and Technology of China (2011CB013105), and in part by the National 863 Project of The Ministry of Science and Technology of China (2011AA03A109).